NASA CONTRACTOR REPORT

NASA CR-137809

A Differential Game Solution to The Coplanar Tail-Chase Aerial Combat Problem

JANUARY 1976

Developed under
CONTRACT No. NAS 2-8844

A. W. Merz

D. S. Hague

Prepared by
AEROPHYSICS RESEARCH CORPORATION
Bellevue, Wash. 98009

FOR THE NATIONAL AERONAUTICS AND SPACE ADMINISTRATION
Ames Research Center, Moffett Field, California 94035

PREFACE

This is the final report incorporating the theory and concluding numerical results of a research study carried out in the period from July to December, 1975, under Contract NAS 2-8844, titled "Study of RPV and MX System Characteristics."

Mr. Michael Tauber was the Technical Monitor for the study, which was done for the Advanced Concepts Branch of the Aeronautics Division, NASA-Ames Research Center. Mr. D. S. Hague, of Aerophysics Research Corporation, served as Project Leader for the study.

TABLE OF CONTENTS

LIST OF FIGURES

A DIFFERENTIAL GAME SOLUTION TO THE

COPLANAR TAIL-CHASE AERIAL COMBAT PROBLEM

A. W. Merz

Aerophysics Research Corporation

1.0 SUMMARY

This report describes the applicable theory and presents the numberical results obtained in a simplified version of the one-on-one aerial combat problem. The principal purpose of the study is the specification of the roles of pursuer and evader as functions of the relative geometry and of the significant physical parameters of the problem. Numerical results are presented for a case in which the slower aircraft is more maneuverable than the faster aircraft.

A third-order dynamic model of the relative motion is described, for which the state variables are relative range, bearing and heading. Certain fundamental results are derived and discussed. An important feature of the present version of the aerial combat model relates to the definition of the end of combat, or "termination." The "tail-chase" end condition requires that the evading aircraft be directly ahead of the pursuer, with the relative headings nearly parallel. The maximum final relative heading angles are arbitrary input parameters, typically equal to about 30^{o}. The ranges at termination are also arbitrary in the present version of the problem, so the weapon systems of both aircraft can be visualized as forward-firing high-velocity weapons, which must be aimed at the tail-pipe of the evader.

It is found that, for the great majority of the relative geometries, each aircraft can evade the weapon system of the other. That is, termination in favor of either aircraft requires that the

angular heading and the angular bearing satisfy certain conditions. Both of these angles change with time as functions of the turn rates of both aircraft. And, though the terminal range is arbitrary, it is impossible for the slower, more maneuverable aircraft or for the faster, less maneuverable aircraft to "get on the tail" of the other, when the initial relative heading exceeds a certain value. This conclusion follows if the evader turns optimally at certain critical times.

While detailed results are presented here for only one set of numerical parameters, the following conclusions are general, and will apply independent of the numerical parameters chosen:

1. Specification of a "capture zone" for each aircraft is possible, by determining combinations of range, bearing and heading for which a tail-chase win is guaranteed regardless of the turn maneuvers chosen by the evader.

2. Pursuit-evasion roles and associated optimal turn maneuvers are given analytically by extremely complex methods, but the results can be approximated "nearly everywhere" by simple "rules of thumb" (e.g., turn into him).

3. Variations in the capture region size and shape can be determined numerically and presented graphically, in order to study the parametric sensitivities to speeds, maximum turn rates and terminal angles-off.

The solution to the problem as presented in this report has required a large amount of interaction between programmer and digital computer, and it is not presently known whether the general numerical problem can be successfully "automated." Only about 30% of various derived candidate maneuver combinations were finally required in the solution displayed here. Of the remainder, any

number might be required for other sets of the parameters (speeds, turn rates, etc.). Furthermore, the theory of differential games is constantly undergoing change, as a result of applying this theory. It is therefore expected that the desired automation will be practical only for "small" parametric variations, an illustrative application of which is given in this report.

2.0 INTRODUCTION

The one-on-one aerial combat problem is the most fundamental version of a more general important guidance and control problem. This is because nearly all actual multi-aircraft combat engagements end as a sequence of one-on-one engagements. That is, an evading aircraft is eventually maneuvering with respect to just one pursuing aircraft, and in the terminal phase of the encounter, both aircraft should be following "one-on-one" control logic. The additional complications of the multi-aircraft encounter are important, of course, but they are ignored at present.

The application of the theory of differential games[1] to the aerial combat problem is important for the following reasons:

1. When termination is uniquely defined, the roles of pursuer and evader should ideally depend only on the initial relative geometry and the performance characteristics of the two aircraft. That is, in an aerial duel which is properly flown by both pilots, neither pilot should switch from a pursuit strategy to an evasion strategy.[2]

2. The optimal maneuvers for both pursuer and evader should also be specified by the relative geometry and the performance capabilities of the aircraft. A choice of maneuvers should occur only when they lead to the same result, as measured by the performance criterion.

3. The significance of a change in aircraft performance parameters (top speed, load factor, etc.) can be measured with respect to its effect on aerial combat performance relative to a specific opponent.

4. New optimal pursuit-evasion tactics for both pilots and RPV autopilots can be expected from the solution to the appropriate differential game model of the problem.

With respect to the first reason given, in both simulated and actual aerial combat engagements, the roles of the pilots may change several times as the encounter progresses. Rational pilots typically want to attack without being attacked, and the mix of offensive-defensive tactics is likely to vary with time, unless the initial geometry is a "set-up" for one pilot or the other. When the initial relative position and heading are such that the roles and maneuvers are obvious, these maneuvers are usually found to be optimal, in the differential games sense. Examples of this type will be discussed in the results given later. Such initial geometries can then be gradually varied until the roles and maneuvers are no longer obvious, and for these geometries, the theory of differential games can be usefully applied to develop both the roles and the associated optimal maneuvers of both aircraft.

As mentioned earlier, actual aerial combat engagements are not usually of the one-on-one type, and it is reasonable to ask if the solution of this simpler problem has relevance to the realistic problem. A satisfactory and convincing answer can be given only by using the results of the study in a simulated or actual multi-aircraft encounter. It is possible, however, that this more complex and realistic application often reduces to a sequence of one-on-one encounters, in which case the derived results should have some relevance. In any case, the solution to the simpler problem is a means of studying performance variations, pursuit-evasion maneuvers and weapon system characteristics, all with respect to a given enemy aircraft.

3.0 MATHEMATICAL MODELLING

The study and analysis of an aerial combat encounter between two aircraft is an extremely difficult problem, which can be approached in two ways:

1. Complex and accurate aircraft simulations can be used with actual or simulated pilot control inputs, to generate experimental and statistical results as to "effective" combinations of aircraft, weapon systems and pursuit-evasion maneuvers[3-10].

2. Simplified models of aircraft dynamics can be coupled with the theory of differential games to specify the roles as functions of the relative geometry and the optimal maneuvers associated with these roles.

These two methods focus on different features of the problem, and both have advantages and shortcomings. The research effort to date has been concentrated on the first approach and a large amount of experimental data has been accumulated. However, it is difficult to draw general conclusions from the data, because of the large number of independent input parameters. Further, the experimental data may deal with a specialized feature of the problem (e.g., a gunsight or thrust-vector control system) without first showing how important this aspect is to the problem solution. However, in any case, the experimental results may be biased by the use of non-optimal control laws. This tends to make suspect any general conclusions based on experiment.

On the other hand, practically all the published theoretical differential game studies have utilized over-simplified or over-specialized mathematical models[13-18] or have dealt with theoretical aspects of differential games[19,20] which are irrelevant to realistic pursuit-evasion problems.

For these reasons, it appears that detailed modelling and subsequent analysis of a portion of the aerial combat system should be done only after it has been shown to have a major impact on the system outcome. This can be demonstrated only by using simplified dynamic models which include what seem to be the fundamental features of the system.

3.1 METHODS OF DEVELOPING TACTICS

The first approach given above has the advantage of permitting practical results to be passed from experienced combat pilots to other pilots and to aircraft designers. Unfortunately, however, the mass of data accumulated in this experimental approach discourages general quantitative conclusions, and it is often impossible to know why a particular combat encounter (simulated or otherwise) ended in favor of one pilot instead of the other. Furthermore, the method tends to be both inefficient and expensive. partly because most of the effects being simulated are secondary to the question of determining which pilot should pursue and which should evade.

The second approach, on the other hand, can be criticized as being too highly idealized with insufficient fidelity in the aircraft maneuver dynamics, and with too little attention given to the transient behavior of the pilots. Nevertheless, the analysis of reduced-order systems in the past has had the effect of isolating the significant parameters, and of permitting a more organized development of improvements in a given system. For this reason, it

is felt that practical low-order versions of the aerial combat problem can be analyzed and solved, in terms of parameters which appear to be of fundamental importance.

In order to validate or to determine limits to this hypothesis, it will be necessary to use results obtained from the simplified model in a realistic simulation of the aerial combat problem. For example, a simulated combat engagement between an "optimally" guided RPV and a comparable aircraft flown by an experienced pilot or guided by approximate combat control laws can demonstrate the value or limitations of the second approach.

3.2 ASSUMPTIONS IN MATHEMATICAL MODEL

All engineering work is based on the analysis of more or less idealized equations describing a certain aspect of the system of interest. If the mathematical details of the study are done correctly, the success and validity of such analyses depend on how well the actual system corresponds to the idealized system. For example, the low-speed small-disturbance stability characteristics of aircraft can be quite accurately determined using linearized equations written for a rigid aircraft. At higher dynamic pressures, on the other hand, aeroelastic effects become significant, and the order and complexity of the equations describing the system increase considerably. But such mathematical refinements in the system equations should be undertaken only after a rather complete study of the simpler equations. In many cases, of course, the higher-ordered equations are never needed, because the aircraft is essentially rigid for practical values of the dynamic pressures.

By analogy, the modelling of the one-on-one aerial combat problem should start with the simplest realistic* dynamic equations which can be used to describe the important features of the motion. After the pursuit-evasion tactics have been found for the simplest mathematical model, refinements can be added to the descriptive equations, and small changes in the results can normally be expected. If the changes in the results are not "small", in the engineering sense of the word, certain important assumptions have been violated. In this case, either the mathematical model must be modified, or the applicability of the results must be restricted to parameters for which such changes are small. For this reason, it is always good practice to emphasize the assumptions and conditions under which a solution has been found. The reader can then judge for himself whether these conditions are reasonable.

The velocities and maximum turn rates of the two aircraft are assumed to be constant during the encounter, to avoid the use of higher-ordered equations of relative motion. This is partially justified by observing that maximum normal accelerations due to lift are usually much larger than axial accelerations due to thrust and drag, except for very high angle of attack configurations. A second justification arises in the analogous problem of developing maritime collision avoidance maneuvers. It is found[21,22] that ship velocities in a hard turn can be reduced by 30% to 50% from their initial values. Nevertheless, the optimal ship turn maneuvers are nearly insensitive to this change in velocity, and excellent results have been obtained by using maneuvers based on the initial velocities of the ships. Of course, any results are perfectly applicable to turn maneuvers which maintain the velocity (or energy) of the aircraft. But, if the direction of a turn maneuver can be shown to be nearly independent of the

* Instantaneous changes in speed or heading require infinite accelerations, and are examples of the use of unrealistic dynamic equations[13-16].

subsequent speed loss, it is irrelevant that the speed is reduced during the turn. In other words, the fundamental purpose of the present study is the development of pursuit-evasion maneuvers, as functions of the relative position and velocity, and not to simulate the transient behavior of the aircraft during these maneuvers.

In the development of pursuit-evasion maneuvers, it will be found useful, if not necessary, to work in terms of retrograde ("backward") time. This is the time-to-go until the end of the combat engagement, which is defined geometrically, in terms of the relative position and heading of the two aircraft. When a suitably simplified model of the aerial combat problem is solved in this way[2,19], it is usually found that the chase is brief and the trajectories rather simple. This provides retroactive justification for certain of the assumptions necessary to the solution. That is, for example, the entire combat time may be so short that the speeds cannot be appreciably altered, so that they can reasonably be considered as constants. However, this behavior may be due to the choice of vehicle parameters in the present study.

The important kinematic characteristics of two aircraft in combat are the vectors describing the relative position and the relative velocity. These two vectors define a plane in which the relative motion occurs, and it is intuitively clear that both aircraft should apply their control accelerations in this plane. This makes the optimal use of the accelerations that each pilot has at his disposal, and if the individual aircraft velocities are also in this plane, an initially planar dynamics problem should remain planar. In fact, experienced combat pilots do attempt to orient their lift vector in the plane of the relative position and velocity vectors. This tends to lead to the development of an encounter lying within a twisting plane in three-dimensional space.

3.3 EQUATIONS OF RELATIVE MOTION

Under the simplifying assumptions discussed above, the relative motion is described by three equations, in which the speeds and maximum turn rates are constant parameters. The coordinate system is chosen to be fixed to the faster aircraft A , and in this axis system the relative position (x,y) and the relative heading (H) of the slower aircraft B satisfy the equations

$$\begin{aligned} \dot{x} &= -\omega_A\, y + V_B \sin H \\ \dot{y} &= -V_A + \omega_A\, x + V_B \cos H \\ \dot{H} &= -\omega_A + \omega_B \end{aligned} \tag{3.1}$$

where the turn rates are bounded; i.e., $|\omega_i| \leq \omega_{i_{max}}$, i = A,B.

As shown in Figure 3.1, the relative motion can be expressed in polar coordinates as well, in terms of the relative bearing (ϕ), the angle-off (θ) and the range (r). The equations of relative motion in these coordinates are:

$$\begin{aligned} \dot{r} &= V_B \cos\theta - V_A \cos\phi \\ \dot{\phi} &= -\omega_A + (V_B \sin\theta + V_A \sin\phi)\ /r \\ \dot{\theta} &= \omega_B - (V_B \sin\theta + V_A \sin\phi)\ /r \end{aligned} \tag{3.2}$$

The two sets of coordinates are related by

$$x = r \sin\phi \ , \ y = r \cos\phi \ , \ H = \phi + \theta . \tag{3.3}$$

The differential equations of motion in Eq.(3.1) are seen to be linear, whenever ω_A and ω_B are constant, with solutions in terms of trigonometric functions. This is because the aircraft are then describing simple circular arc paths in fixed coordinates. The equations are solved by first determining the heading as a linear function of time, and by then solving the position equations by standard methods. The more symmetrical polar equations in (3.2), however, can be solved only in terms of arc tangent functions. These equations show how the angles ϕ and θ depend upon both the aircraft turn rates and the kinematics of the problem. When the range is large, $\dot{\phi} \cong -\omega_A$ and $\dot{\theta} \cong \omega_B$, but otherwise, highly nonlinear effects can predominate. Thus, at large ranges A can control the bearing, but B can control the angle-off! Since the bearing and angle-off of A relative to B are $\pi - \theta$ and $\pi - \phi$, respectively, this geometric symmetry means that aircraft at an initially large distance from each other will often null the steering errors and turn the initial encounter into a head-on pass with little lateral offset. However, short-range maneuvers are far more complex.

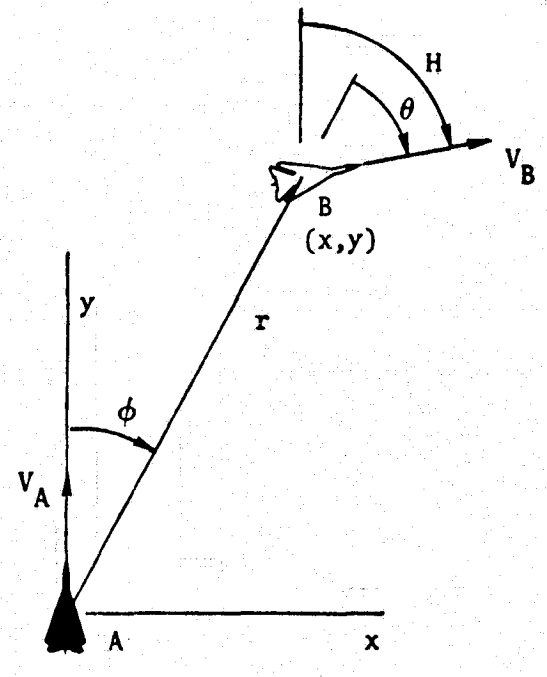

Figure 3.1 Relative Motion Coordinates

The solutions to Eq.(3.1) are given here in terms of the final (terminal) conditions (x_f, y_f, H_f). For constant values of the two turn rates, both aircraft describe circular arcs in real space, and B's position relative to A is given by the following functions of the retrograde time, τ:

$$x = x_f \cos\tau + \omega_A(1 - \cos\tau + y_f \sin\tau) + V_B/\omega_B \left[\cos(H_f + \omega_A \tau) - \cos H\right]$$

$$y = y_f \cos\tau + (1 - \omega_A x_f) \sin\tau - V_B/\omega_B \left[\sin(H_f + \omega_A \tau) - \sin H\right]$$

$$H = H_f + (\omega_A - \omega_B)\tau \,, \quad |\omega_i| \leq \omega_{i_{max}} \,, \quad i = A, B \qquad (3.4)$$

Here, the velocity of the faster aircraft has been normalized to $V_A = 1$, and the maximum turn rate of this aircraft is normalized to $\omega_{A_{max}} = 1$. This means that the unit of distance in the normalized equations is the turn radius of aircraft A. For brevity, the maximum turn rate of the slower aircraft is written as $\omega_{B_{max}} = \omega$, which will be assumed greater than 1, while B's velocity is $V_B < 1$. The slower aircraft (B) is therefore assumed to be more maneuverable than the faster aircraft (A). This will be the case, for example, if the turns are made at the same load factor, so that the product of speed and maximum turn rate is constant for both aircraft.

4.0 PURSUIT-EVASION MANEUVER DETERMINATION

The equations of coplanar relative motion derived in the previous section provide a dynamic model of the aerial combat problem, in terms of a small number of parameters and dynamic variables. From the points of view of the aircraft pilots, the solution to the combat problem should give the roles and the maneuvers of both pilots as functions of the relative geometry. This is also the point of view taken here where, however, it is necessary to investigate the more subtle dependence of the optimal maneuvers on the aircraft velocities and maximum turn rates, which obviously lead to time variations in the relative geometry.

The method of solution to the role-determination problem is based on the concept of the "barrier"[1]. This is a surface in the state space on which optimal trajectories occur which correspond to the "near-miss" or "simultaneous kill" trajectories in real space. The simplest interpretation to be given to the barrier is the following: If the evador is located slightly "outside" the local barrier, he can maneuver so as to avoid the pursuer indefinitely. On the other had, if he is just inside the barrier, and the pursuer maneuvers optimally, no escape by the evader is possible.

By letting both A and B take the role of pursuer, two barriers are found, both of which can be shown in axes fixed to A. In the simplest case, these barriers do not intersect and they bound two separate regions of the state space. Even if they intersect, other considerations show that two regions in the state space exist, which are those relative positions corresponding to the following outcomes:

1. A wins if A maneuvers optimally, regardless of B's maneuvers.
2. B wins if B maneuvers optimally, regardless of A's maneuvers.

A third region may also exist, which is "outside" both of these two regions, in which both A and B can evade the other indefinitely, regardless of the maneuvers used by the pursuer.

4.1 TERMINAL CONDITIONS

Termination in an aerial combat encounter can be defined in many different ways, all of which mean that the differential game has ended. A conflict exists, however, between the complex limitations of current air-to-air weapon systems and the requirements of relative simplicity in the mathematical models of these systems. The terminal conditions are actually functions of many independent physical quantities, but for the purposes of this report, they must be defined in much simpler terms, in order to lead to a problem definition which is both practical and soluble.

In the present report, attention is focused on the tail-chase or heading-limited end condition, in which the evader (A or B) is directly ahead of the pursuer, with a "near-parallel" heading. These terminal configurations are shown in Figure 4.1 for both A and B pursuing the other. The relative terminal heading or "angle-off" is measured clockwise from A's velocity to B's velocity, and this angle must be smaller in magnitude than H_A or H_B (depending on the roles).

The angular parameters H_A and H_B, are expected to have values of approximately 10^o-30^o. These would actually depend on the details of the gun-sight or missile guidance system used by the aircraft. The range at termination can also be an important factor in the realistic modelling of the aerial combat problem, but in the present application, the final range is considered as irrelevant. This is consistent with the assumption that the forward-firing weapons of both aircraft have "long-range" guidance systems which can follow any subsequent evasive maneuvers of the target. A more detailed model of the problem would also include the final angular bearing as a parameter; instead of requiring that the evader be exactly

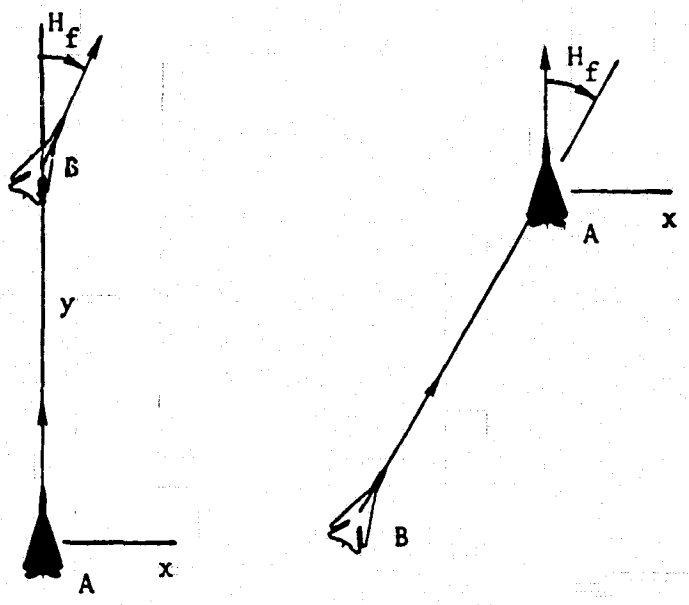

a) A pursues, B evades

$x_f = 0$

$y_f \geq 0$

$|H_f| \leq H_A$

b) B pursues, A evades

$x_f = y_f \tan H_f$

$y_f \leq 0$

$|H_f| \leq H_B$

Figure 4.1 Heading-Limited Terminal Conditions in A's Axis System

ahead of the pursuer at the end of the chase. In this case, too, it is felt that sufficient complexity already exists in the problem statement and that any generalization of this kind can be postponed for the present. It might also be suggested that both the terminal bearing and the terminal bearing rate be zero, to allow for target tracking requirements. This generalization obviously has practical importance, but it also must await the solution to the present simpler problem.

4.2 OPTIMIZATION CRITERIA AND NECESSARY CONDITIONS

The principal results being sought in this analysis are the sets of initial conditions for which a win is guaranteed for the pursuer, regardless of the maneuvers used by the evader. The pursuer, of course, can be either aircraft A or B, and it is expected that the "capture regions" of A and B will intersect on those surfaces which separate the two regions. That is, the state space, as described by the vector (x, y, H), will be composed of at most three regions, corresponding to wins by A or B, and to a "stand-off" or escape by the faster aircraft. For other values of the parameters (e.g., if the faster aircraft is also more maneuverable) the third or "escape" region may be absent, and one or the other aircraft must win for all initial conditions.

The capture region of either aircraft is determined by a consideration of the family of "barrier"[1] trajectories. This family of trajectories forms a "semi-permeable surface", which prevents the state from crossing the surface as long as both aircraft maneuver optimally in its neighborhood. Along the paths on this surface, the pursuit-evasion roles are known, and the trajectories end in a "near-miss" or simultaneous kill configuration.

(For the weapon models used here, a simultaneous kill is actually a collision with near-parallel headings.) The reasoning is that a small displacement normal to the barrier means a clear win or a clear escape by the pursuer or evader, respectively. Therefore, the pursuer's semi-permeable surface locally divides the state space into capture and escape regions, for the assumed roles. But, a different set of barrier trajectories exists for the reversed-role assumption and when the two barriers intersect, one or the other must be discontinued. An exception occurs on the "collision" barrier, which is itself a role-reversal locus. These notions are illustrated in Figure 4.2.

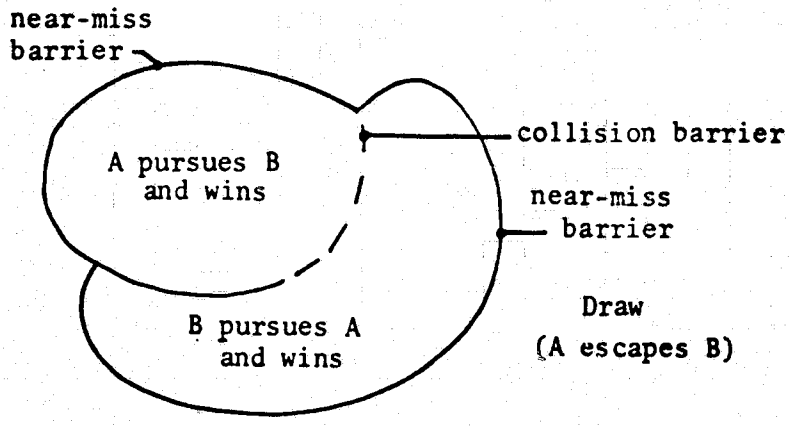

Figure 4.2 Conceptual Division of State Space

The pursuit-evasion game can be given a positive value if B wins, and a negative value if A wins, where "winning" is defined for A and B by a terminal configuration in favor of either, as shown in Figure 4.1. The value of the game for trajectories following the barrier is therefore zero, and this

value function has a total time derivative along the optimal trajectories which is also zero. This is the "Main Equation" of Isaacs[1], which takes the following form,

$$\min_{\omega_A} \max_{\omega_B} [\, \lambda_x \dot{x} + \lambda_y \dot{y} + \lambda_H \dot{H} \,] = 0$$

Substituting from Eq.(3.1) with $V_A = 1$,

$$\begin{aligned} \min_{\omega_A} \max_{\omega_B} [\, & \lambda_x(-\omega_A y + V_B \sin H) \\ & + \lambda_y(-1 + \omega_A x + V_B \cos H) \\ & + \lambda_H(-\omega_A + \omega_B)] = 0 \end{aligned} \tag{4.1}$$

4.2.1 ADJOINT EQUATIONS AND OPTIMAL MANEUVERS

The adjoint vector, $\nabla\lambda = (\lambda_x, \lambda_y, \lambda_H)$ consists of partial derivatives of the payoff function, for which a saddle-point solution is sought. These variables obey a set of linear differential equations, which are found by differentiating Eq.(4.1) with respect to time:

$$\begin{aligned} \dot{\lambda}_x &= -\omega_A \lambda_y \\ \dot{\lambda}_y &= \omega_A \lambda_x \\ \dot{\lambda}_H &= V_B (\lambda_y \sin H - \lambda_x \cos H) \end{aligned} \tag{4.2}$$

When A is turning hard right or left, $\omega_A = \pm 1$, and the retrograde solutions to these equations are expressed in terms of the final values of the adjoints and the time-to-go, τ:

$$\lambda_x = \lambda_{x_f} \cos\tau + \lambda_{y_f} \sin\omega_A\tau$$

$$\lambda_y = -\lambda_{x_f} \sin\omega_A\tau + \lambda_{y_f} \cos\tau \qquad (4.3)$$

$$\lambda_H = \lambda_{H_f} + V_B/\omega_B \left[\lambda_{x_f}(\sin H_f - \sin(H_f - \omega_B\tau)) + \lambda_{y_f}(\cos H_f - \cos(H_f - \omega_B\tau))\right]$$

It will be shown that the terminal values of the adjoints are derivable from the geometric conditions at the final time, when $\tau = 0$.

The optimization procedure implied in Eq.(4.1) gives the turn-rate controls of both pilots as functions of the current values of the state and adjoint variables;

$$\omega_A = \omega_{A_{max}} \operatorname{sgn} S_A = \operatorname{sgn} S_A$$

$$S_A = \lambda_x y - \lambda_y x + \lambda_H$$

and

$$\omega_B = \omega_{B_{max}} \operatorname{sgn} S_B = \omega \operatorname{sgn} S_B \qquad (4.4)$$

$$S_B = \lambda_H$$

where the switch functions of A and B are denoted S_A and S_B respectively.

The optimal maneuvers for both aircraft are therefore hard turns to left or right unless the switch function is identically zero. In this case, it can be shown that the corresponding optimal maneuver is a "dash" or straight path, for which the turn rate is zero. Thus, regardless of the relative geometry or performance characteristics of the aircraft, only nine maneuver pairs (3 maneuvers for each of 2 aircraft) are candidates for optimal controls in this model of the aerial combat problem.

4.2.2 END CONDITIONS

The optimal maneuvers can be computed only when the switch functions are known, which requires that the adjoints be known. Boundary conditions on the adjoints, however, are known only at the time of termination, when the geometry corresponds to the "near-miss" or "collision" end condition. Further analysis therefore requires consideration of the relative motion which precedes the barrier end conditions.

The barrier trajectories which precede these end conditions are of two general types:

1. "Near miss" trajectories for which the evader contacts tangentially the edge of the pursuer's capture region,
2. "Collision" trajectories, for which "wins" occur simultaneously for both aircraft.

These trajectories are representative solutions to the game of kind[1], which separate "capture" from "escape", and which are illustrated for the tail-chase end condition in reference 23.

Parameters H_A and H_B were defined in Figure 4.1, and are shown in a perspective drawing of the two capture regions in Figure 4.3. These relative heading angles in the tail-chase end condition bound a two-dimensional region in the relative space on which capture must occur, and it is seen that the near-miss trajectories contact the capture regions either along the edges or tangentially along the surfaces. The collision trajectories occur at $x = y = 0$, along a line segment which is common to both capture regions.

Trajectories in this 3-space (x, y, H) are continuous curved paths obeying the equations of relative motion. That is, the relative "velocity" has components $\dot{x}$, $\dot{y}$, and $\dot{H}$, and the trajectories are smooth except where A or B switches turn directions.

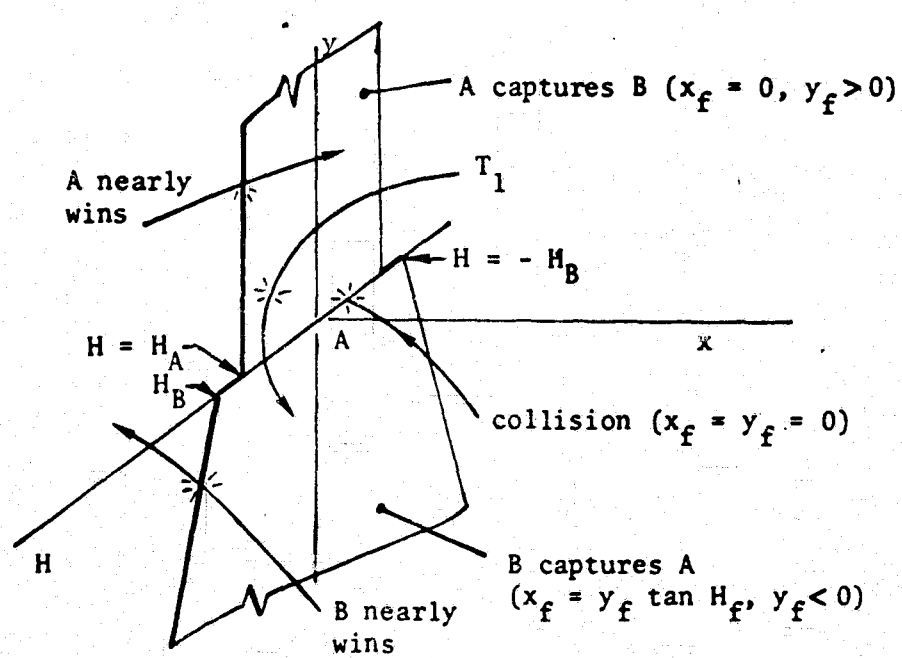

Figure 4.3 Terminal Trajectories on the Barrier for the Tail Chase End Condition

Depending on the relative orientation and turn maneuvers of the aircraft, 16 different terminal configurations are possible in this model of the problem, of which three are discussed in detail in reference 23. The other cases are listed in Table I, where it is seen that more stringent inequalities can occur in the applicable range of the independent variable. These inequalities can be derived by the requirement that neither switch function changes sign while the heading changes (retrogressively) from H_f to H. Further discussion of these maneuvers is postponed to Section 5.0.

4.2.3 SWITCH CONDITIONS

The retrograde integration of the state and adjoint equations allows the switch functions of both A and B to be written in terms of the terminal values of state and adjoint vectors, and the associated turn rates ω_A and ω_B. In these expressions, the independent variable is the "time-to-go" until the near miss or collision occurs. It is denoted by the symbol $\tau = t_f - t$, where t_f is the time at which the near miss or collision occurs.

By combining the results presented in Eqs. (3.4) and (4.3), the switch functions for aircraft A and B can be expressed in retrograde time as

$$S_A = \lambda_{x_f}(y_f + \sin\tau) - \lambda_{y_f}[x_f - \omega_A(1 - \cos\tau)] + \lambda_{H_f}$$

$$S_B = \lambda_{H_f} + \frac{V_B}{\omega_B}[\lambda_{x_f}(\sin H_f - \sin(H_f - \omega_B\tau)) + \lambda_{y_f}(\cos H_f - \cos(H_f - \omega_B\tau))] \tag{4.7}$$

where $\omega_A = \text{sgn } S_A = \pm 1$ and $\omega_B = \omega \text{ sgn } S_B = \pm\omega$.

TABLE I

OPTIMAL PURSUIT-EVASION TERMINAL MANEUVERS

(Heading-Limited End Condition)

Case	Turns	Terminal State (x_f, y_f, H_f)	Terminal Adjoint $(\lambda_{x_f}, \lambda_{y_f}, \lambda_{H_f})$
1	$A_R B_R$	$(0, 0, H_f)$ $-\cos^{-1} V_B \le H_f \le 0$	$(\sin\beta, \cos\beta, 0)$ $\tan\beta = \dfrac{1-V_B \cos H_f}{V_B \sin H_f}$
2	$A_R B_L$	$(0, 0, H_f)$ $-H_B \le H_f \le -\cos^{-1} V_B$	$(\sin\beta, \cos\beta, 0)$ $\tan\beta = \dfrac{1-V_B \cos H_f}{V_B \sin H_f}$
3	$A_R B_R$	$(0, V_B \sin H_f, H_f)$ $0 \le H_f \le H_A$	$(1, 0, 0)$
4	$A_R B_R$	$(0, y_f, H_A)$ $0 \le y_f \le y_1^*$ $V_B \sin H_A \le y_f$	$(\cos\beta, 0, \sin\beta)$ $\tan\beta = \dfrac{V_B \sin H_A - y_f}{1-\omega}$ $\tan\beta = \dfrac{-V_B \sin H_A + y_f}{-1+\omega}$
5	$A_L B_R$	$(0, y_f, H_A)$ $y_f \ge y_2^{**}$	$(\cos\beta, 0, \sin\beta)$ $\tan\beta = \dfrac{y_f + V_B \sin H_A}{-1-\omega}$
6	$A_L B_L$	$(0, 0, H_f)$ $0 \le H_f \le \cos^{-1} V_B$	$(\sin\beta, \cos\beta, 0)$ $\tan\beta = \dfrac{-1 + V_B \cos H_f}{-V_B \sin H_f}$
7	$A_L B_R$	$(0, 0, H_f)$ $\cos^{-1} V_B \le H_f \le H_B$	$(\sin\beta, \cos\beta, 0)$ $\tan\beta = \dfrac{-1 + V_B \cos H_f}{-V_B \sin H_f}$

Table I

(continued)

Case	Turns	Terminal State (x_f, y_f, H_f)	Terminal Adjoint $(\lambda_{x_f}, \lambda_{y_f}, \lambda_{H_f})$
8	$A_L B_L$	$(0, \ V_B \sin H_f, \ H_f)$ $-H_A \leq H_f \leq 0$	$(-1, \ 0, \ 0)$
9	$A_L B_L$	$(0, \ y_f, \ -H_A)$ $0 \leq y_f \leq y_1^*$ $y_f \geq V_B \sin H_A$	$(\cos\beta, \ 0, \ \sin\beta)$ $\tan\beta = \dfrac{V_B \sin H_A - y_f}{-1 + \omega}$ $\tan\beta = \dfrac{-V_B \sin H_A + y_f}{1 - \omega}$
10	$A_R B_L$	$(0, \ y_f, \ -H_A)$ $y_f \geq y_2^{**}$	$(\cos\beta, \ 0, \ \sin\beta)$ $\tan\beta = \dfrac{-y_f - V_B \sin H_A}{1 + \omega}$
11	$B_L A_L$	$(-\sin^2 H_f/\omega, -\sin H_f \cos H_f/\omega, H_f)$ $0 \leq H_f \leq H_B$	$(-\cos H_f, \sin H_f, -\sin H_f/\omega)$
12	$B_L A_L$	$(y_f \tan H_B, \ y_f, \ H_B)$ $-\sin H_B \cos H_B/\omega \leq y_f \leq 0$ $y_f \leq -\sin H_B \cos H_B$	$(\cos\beta\cos H_B, \ -\cos\beta \sin H_B, \ \sin\beta)$ $\tan\beta = \dfrac{-\sin H_B - y_f/\cos H_B}{-\omega + 1}$ $\tan\beta = \dfrac{\sin H_B + y_f/\cos H_B}{\omega - 1}$
13	$B_R A_L$	$(y_f \tan H_B, \ y_f, \ H_B)$ $y_f \leq -\sin H_B \cos H_B$	$(\cos\beta\cos H_B, \ -\cos\beta \sin H_B, \ \sin\beta)$ $\tan\beta = \dfrac{-\sin H_B - y_f/\cos H_B}{\omega + 1}$
14	$B_R A_R$	$(\sin^2 H_f/\omega, \sin H_f \cos H_f/\omega, H_f)$ $-H_B \leq H_f \leq 0$	$(\cos H_f, \ -\sin H_f, \ -\sin H_f/\omega)$

Table I

(continued)

Case	Turns	Terminal State (x_f, y_f, H_f)	Terminal Adjoint $(\lambda_{x_f}, \lambda_{y_f}, \lambda_{H_f})$
15	$B_R A_R$	$(-y_f \tan H_B,\ y_f,\ -H_B)$ $-\sin H_B \cos H_B/\omega \le y_f \le 0$ $y_f \le -\sin H_B \cos H_B$	$(\cos\beta \cos H_B,\ \cos\beta \sin H_B, -\sin\beta)$ $\tan\beta = \dfrac{-\sin H_B - y_f/\cos H_B}{\omega - 1}$ $\tan\beta = \dfrac{\sin H_B + y_f/\cos H_B}{-\omega + 1}$
16	$B_L A_R$	$(-y_f \tan H_B,\ y_f,\ -H_B)$ $y_f \le -\sin H_B \cos H_B$	$(\cos\beta \cos H_B,\ \cos\beta \sin H_B, -\sin\beta)$ $\tan\beta = \dfrac{-\sin H_B - y_f/\cos H_B}{-\omega - 1}$

* $y_1 = \dfrac{1}{\omega}\left[V_B \sin H_A - (\omega - 1)\sin\left(\dfrac{H_A - H}{\omega - 1}\right)\right]$

** $y_2 = \dfrac{1}{\omega}\left[V_B \sin H_A - (\omega + 1)\sin\left(\dfrac{H_A - H}{\omega + 1}\right)\right]$

For specific terminal ranges, singular arcs for both A and B can precede the maneuvers given in cases 12 and 15.

Singular arcs cannot occur just prior to termination, because this would imply

$$S_A = \lambda_x y - \lambda_y x + \lambda_H = \dot{S}_A = \lambda_x = 0$$

or

$$S_B = \lambda_H = \dot{S}_B = V_B (\lambda_x \cos H - \lambda_y \sin H) = 0 \qquad (4.8)$$

and neither of these conditions can hold at t_f. This would mean that all adjoints are zero. Such a situation can arise only if the outcome, as measured by the performance criterion, is independent of the state and its rate of change. This degenerate case is excluded from the mathematical model being used for the aerial combat problem.

Because the backwards trajectories are most easily parametrized at specified (constant) values of heading, H, the solution to the heading equation (using the appropriate controls) is found as

$$H = H_f + (\omega_A - \omega_B) \tau \qquad (4.9)$$

This expression gives the time-to-go, τ, when H and H_f are known, and therefore both switch functions can be calculated to assure that neither has changed sign during the retrograde trajectory of interest.

More generally, when both state and adjoints are known at t_f, the times (if any) at which S_A and S_B equal zero can be derived in terms of trigonometric arc-functions. For example, the representative case 12 from Table I can be chosen (because the less maneuverable aircraft never switches while pursuing), and for $y_f \leq -\sin H_B \cos H_B$, with both A and B turning left, the switch functions are

$$S_A = \omega (\sin H_B + y_f / \cos H_B) - (\omega - 1) \sin (H_B - \tau) \ .$$

$$S_B = \sin H_B + y_f / \cos H_B + V_B \left(\frac{\omega - 1}{\omega}\right) \sin \omega\tau \quad . \tag{4.10}$$

When equated to zero, these can be solved for the retrograde-switch times,

$$\tau_A = H_B + \sin^{-1}\left[\frac{-\omega (\sin H_B + y_f/\cos H_B)}{\omega - 1}\right]$$

$$\tau_B = \frac{1}{\omega} \sin^{-1}\left[\frac{-\omega (\sin H_B + y_f/\cos H_B)}{V_B (\omega - 1)}\right] \tag{4.11}$$

Since the independent variable here is y_f, it follows that no switch occurs if the argument of the arcsin function exceeds 1 in magnitude; i.e., neither switches if the terminal range is large enough.

4.2.4 GAP CLOSURE CONDITION

A detail of the solution which is not reported in Ref. 23 relates to the closing of an "angular gap". This gap turns out to be of great importance in the development of a complete solution to the problem of role-determination. Furthermore, other details of the solution, as reported in Sec. 4.2.4 to 4.2.6 of Ref. 23, appear to be unnecessary for the aircraft parameters which have been chosen. Consequently, this final report emphasizes the significance of the gap closure condition by describing how it is obtained.

At the corner of a capture region, trajectories can arrive from at least two different directions, as shown schematically in Fig. 4.4. This illustrates the qualitative situation which holds at the point, $\underline{x}_f = (0, 0, H_A)$. It is seen that the maneuvers $A_R B_R$ (Case 4) have y_f as a parameter, while the maneuvers $A_L B_L$ (Case 6) have H_f as a parameter. It is also seen that the paths which arrive at the final point from opposite sides must be connected by a surface which is generated by two-part paths.

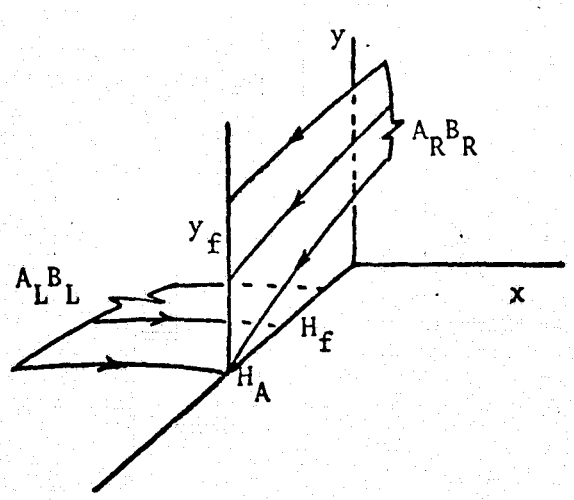

Fig. 4.4 - Geometry of Gap at $(0, 0, H_A)$

The terminal adjoints in case 4 are $(\lambda_{x_f}, 0, \lambda_{H_f})$, where $\lambda_{H_f} > 0$, while in case 6, they are $(\lambda_{x_f}, \lambda_{y_f}, 0)$, where $\lambda_{y_f} < 0$.

To close the gap with optimal trajectories, a parameter p will be varied in the range 0 to 1, such that the terminal adjoint is expressible as

$$\underline{\lambda}_f = (a, -p, 1-p)$$

Now, an examination of the retrograde heading variation in Fig. 4.5 shows that the trajectory can have 0, 1, or 2 switches as the heading varies from H to H_A, depending both upon the heading H and the values of the switch times τ_A and τ_B. Expressions are required for these switch times, and for this purpose, the Hamiltonian is written at termination for the maneuvers $A_R B_R$, which is equivalent to the following equation for a(p):

$$a\, V_B\, sH_A = p(-1 + V_B\, cH_A) - (1-p)(\omega - 1)$$

The retrograde switch times for A and B are then found by solving

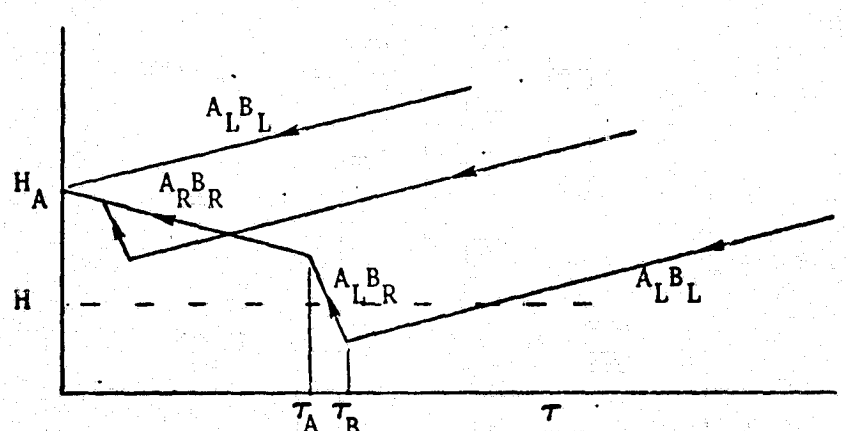

Fig. 4.5 Heading Variations with Retrograde Time

the corresponding switch function equations, which are

$$S_A(\tau_A) = as\tau_A + pc\tau_A + 1 - 2p = 0$$

and

$$S_B(\tau_B) = 1 - p + (V_B/\omega)[a(sH_A - s(H_A - \omega\tau_B)) - p(cH_A - c(H_A - \omega\tau_B))] = 0$$

After some effort, the switch times are then expressed as

$$s\tau_A = \frac{-a(1-2p) + p[a^2 + p^2 - (1-2p)^2]^{\frac{1}{2}}}{a^2 + p^2}$$

$$s\omega\tau_B = \frac{-AC + B[a^2 + p^2 - C^2]^{\frac{1}{2}}}{a^2 + p^2}$$

where

$$A = psH_A + acH_A$$

$$B = pcH_A - asH_A$$

$$C = asH_A - pcH_A + \omega(1-p)/V_B$$

These rather ungainly equations have been applied for only one set of parameters, for which it was found that $\tau_A < \tau_B$, and for which only the first (retrograde) intersection shown in Fig. 4.5 was significant. General conclusions as to the conditions under which these equations are applicable are therefore not available. For the numerical parameters illustrated in Fig. 5.1, however, the barrier segments of interest are those labelled $A_{RL}B_L$ and $A_{LR}B_R$ at the relative headings H = 0°, 10°, 20° and 25°.

5.0 NUMERICAL EXAMPLE OF ROLE-DETERMINATION

The concepts and equations of the earlier portions of this report have been applied to a specific set of aircraft parameters, and capture regions for both aircraft have been found. The numerical values of the parameters chosen for this example are:

$$V_A = 1.0, \qquad \omega_{A_{max}} = 1.0, \qquad H_A = 30^o$$

$$V_B = .5, \qquad \omega_{B_{max}} = 1.1, \qquad H_B = 40^o$$

and the slower aircraft B is seen to be slightly more maneuverable than aircraft A. Also, it may be noted that A's weapon system requires the terminal headings to be more nearly parallel, since $H_A < H_B$. In the results to be discussed, the unit of distance is the turn radius of aircraft A (V_A/ω_A), In these units, which might correspond to a physical distance of a mile or more, B's minimum turn radius is considerably smaller, $V_B/\omega_B \simeq .4545$.

The capture boundary results are shown graphically in Figure 5.1, and the following details are noteworthy:

1. A total of 14 different maneuver combinations are required to define the barriers, which include several 2-part maneuvers. These correspond to cases

   1, 4a, 5, 6, 9a, 10, 12, 12b, 12ab, 13, 15b, 15ab, 16 and 16a,

   where "a" and "b" are used to indicate retrograde switches by A or B, respectively. That is, e.g., Case 12 corresponds to $B_L A_L$ (Table I), Case 12b to $B_{RL} A_L$, and Case 12ab to $B_{RL} A_{RL}$.

2. A can win only if $H<H_A = 30^o$, since $\omega_A<\omega_B$. That is, if the heading is initially greater than H_A, B can prevent its subsequent reduction to this value, regardless of A's turns.

3. For the great majority of relative positions both A and B can evade the other indefinitely. This is because B cannot control both the heading and the bearing at all ranges. That is, when the range is large enough, A's speed allows him to control the bearing, as implied by equation (3.2).

4. The optimal turn maneuvers can often, but not always, be expressed as "turn toward him", whether pursuing or evading. For example, when $H = 0^o$, each initially turns toward the other except (i) when A and B are nearly side by side; here A initially turns away from B, and (ii) when the barrier is a collision trajectory, for which B turns away from A. Other exceptions occur at other relative headings.

5. Single-stage near-miss maneuver loci are always straight lines.

The terminal maneuvers B_RA_L (case 13) have zero time-duration when $H = 40^o$, and this locus for $H>40^o$ is extended by the barrier corresponding to the maneuvers B_LA_L (case 12). Both of these straight loci are extended by the curved locus corresponding to $B_{RL}A_L$.

The results shown in Figure 5.1 together with their antisymmetric counterparts (for $H<0^o$) define two closed "volumes" in the three-dimensional relative state space. These volumes are of semi-infinite extent for $H<45^o$ only because the ranges of the weapons have been assumed infinite. As shown in Figure 5.1(a) at $H = 0^o$, for example, the region far ahead of A should be bounded at some finite range comparable to A's effective weapon range, depending on the time required for B to increase the relative heading to H_A. Similarly,

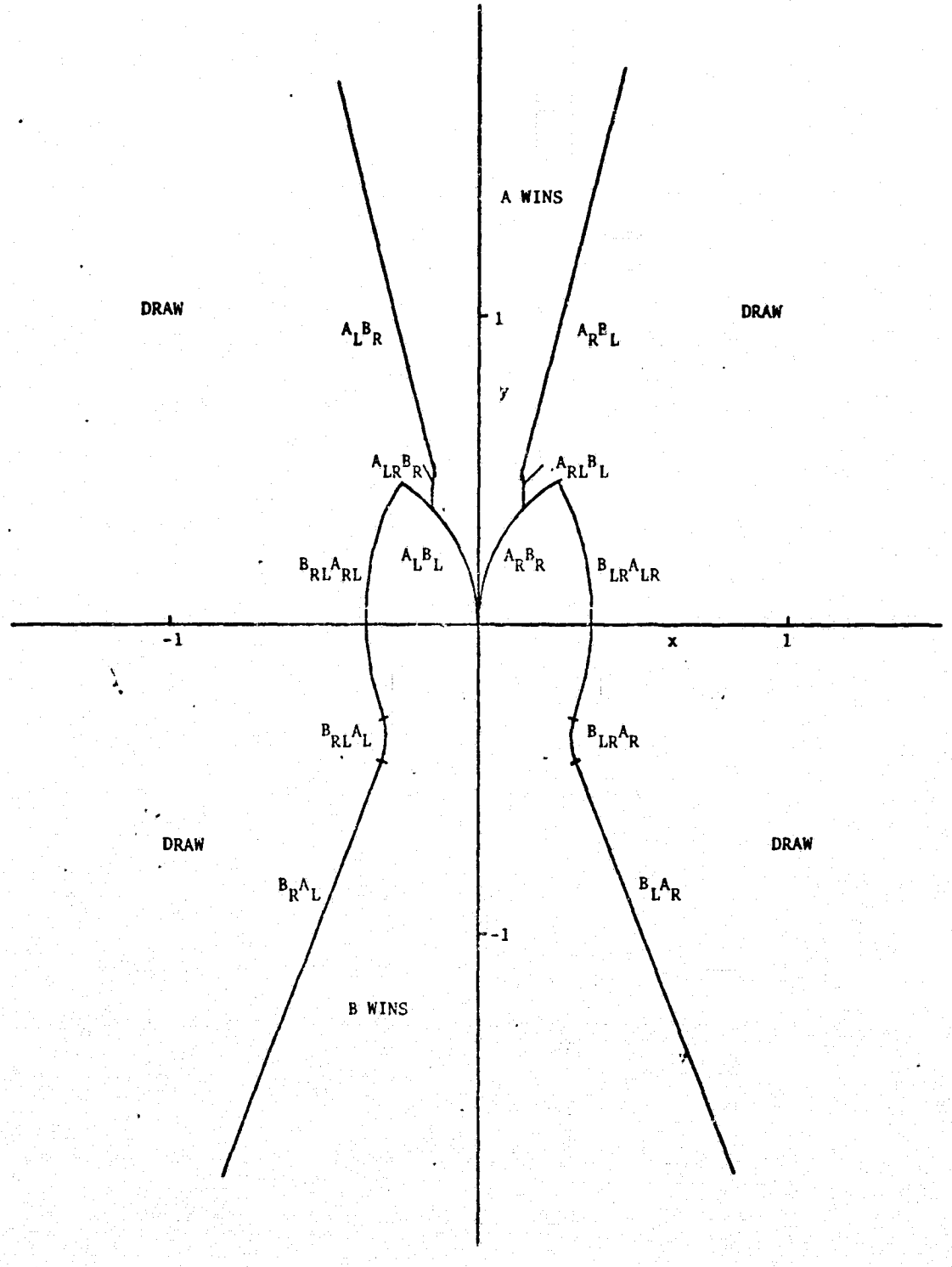

FIGURE 5.1(a). CAPTURE REGIONS, $\overline{H} = 0^{o}$

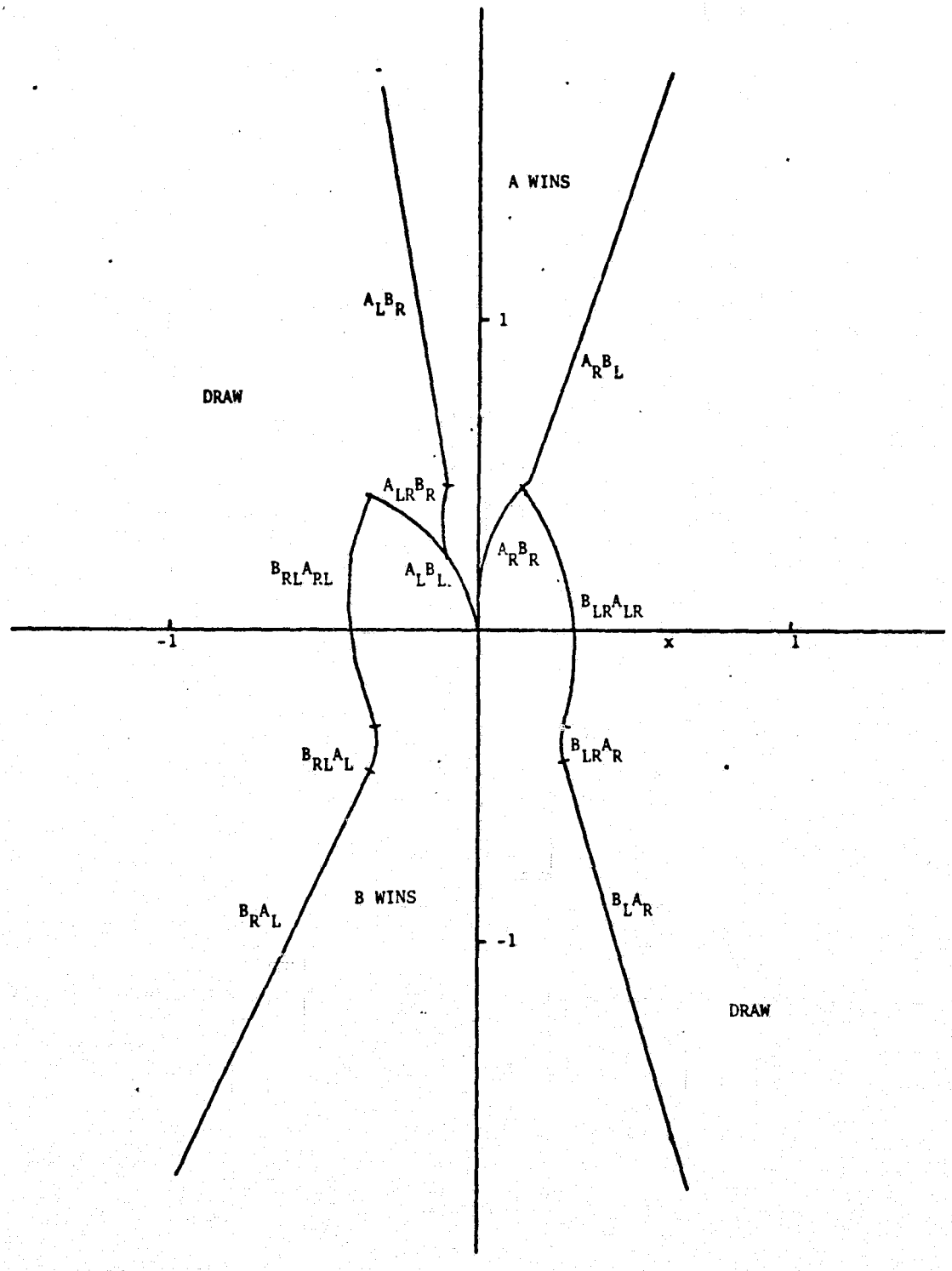

FIGURE 5.1(b). CAPTURE REGIONS, $\overline{H} = 10^{o}$

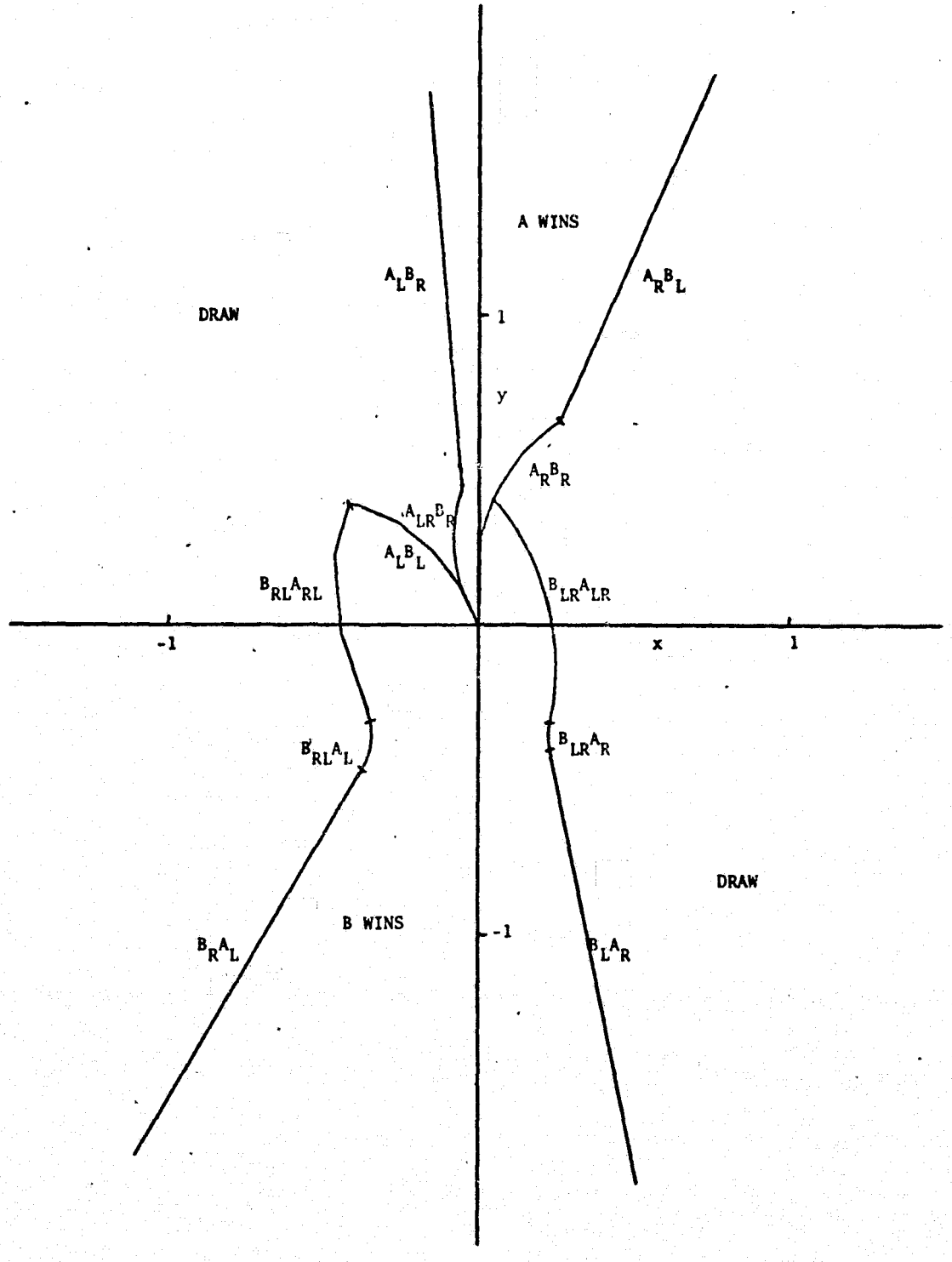

FIGURE 5.1(c). CAPTURE REGIONS, H = 20°

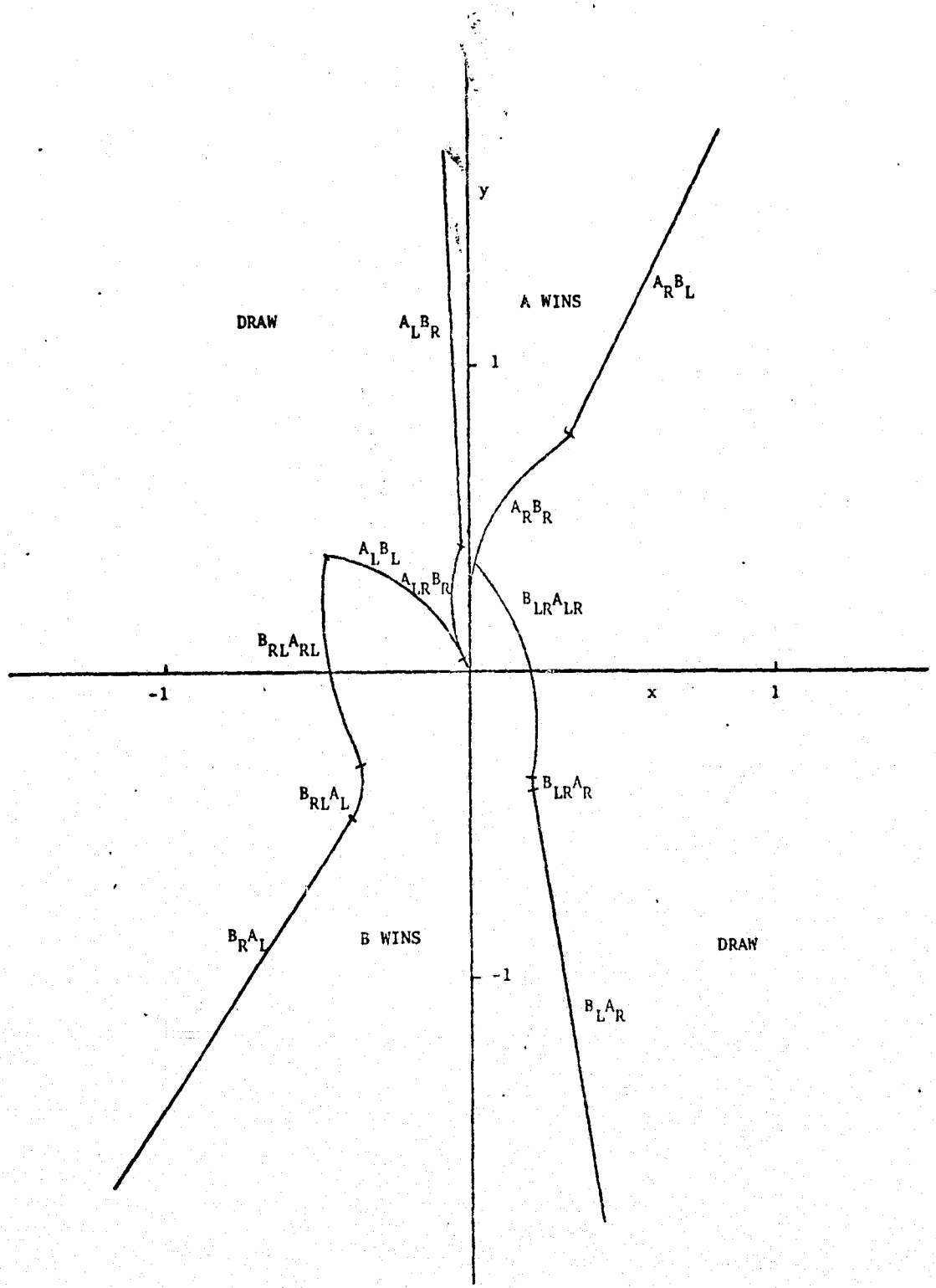

FIGURE 5.1(d). CAPTURE REGIONS, H = 25^o

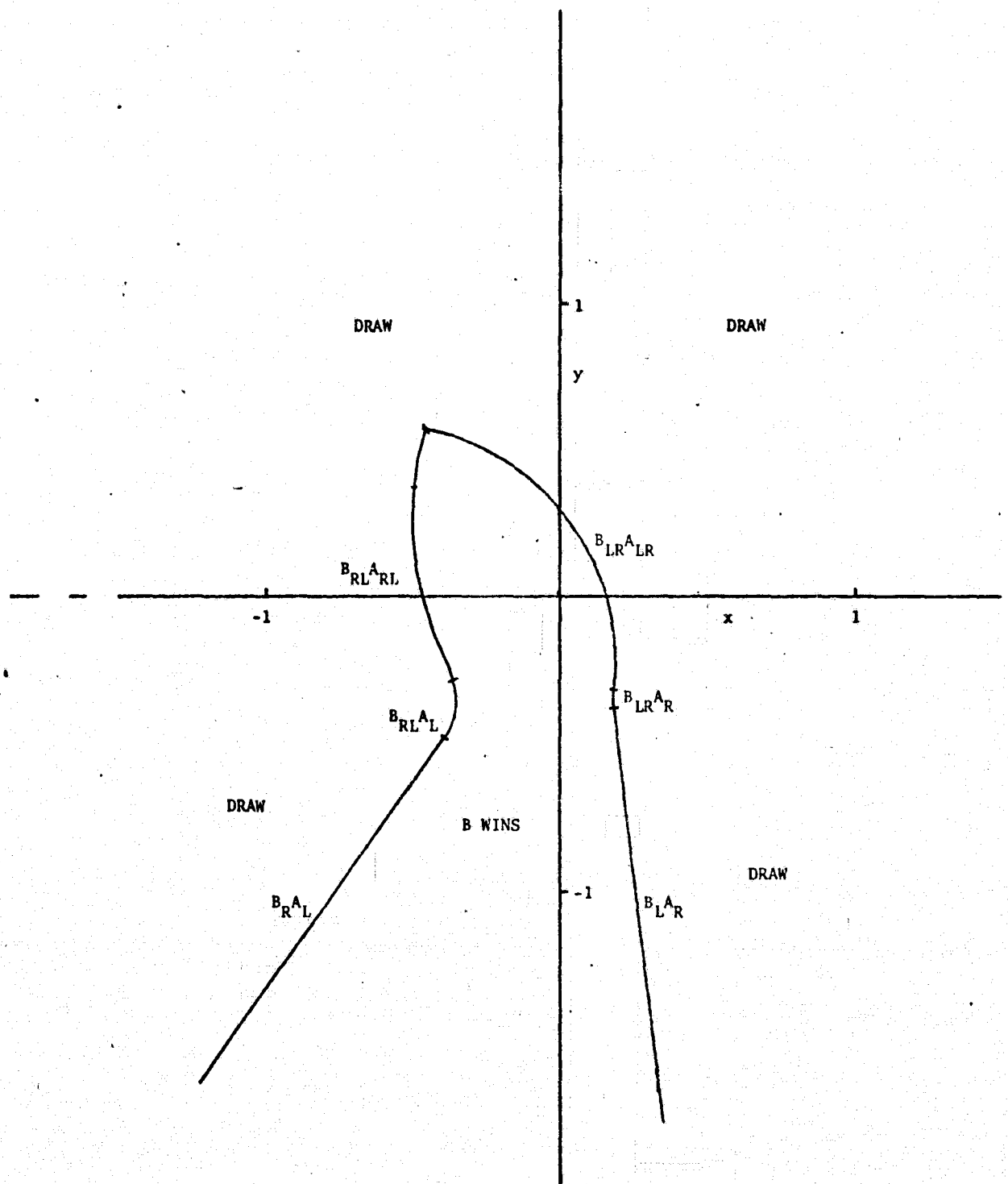

FIGURE 5.1(e). CAPTURE REGIONS, H = 30^o

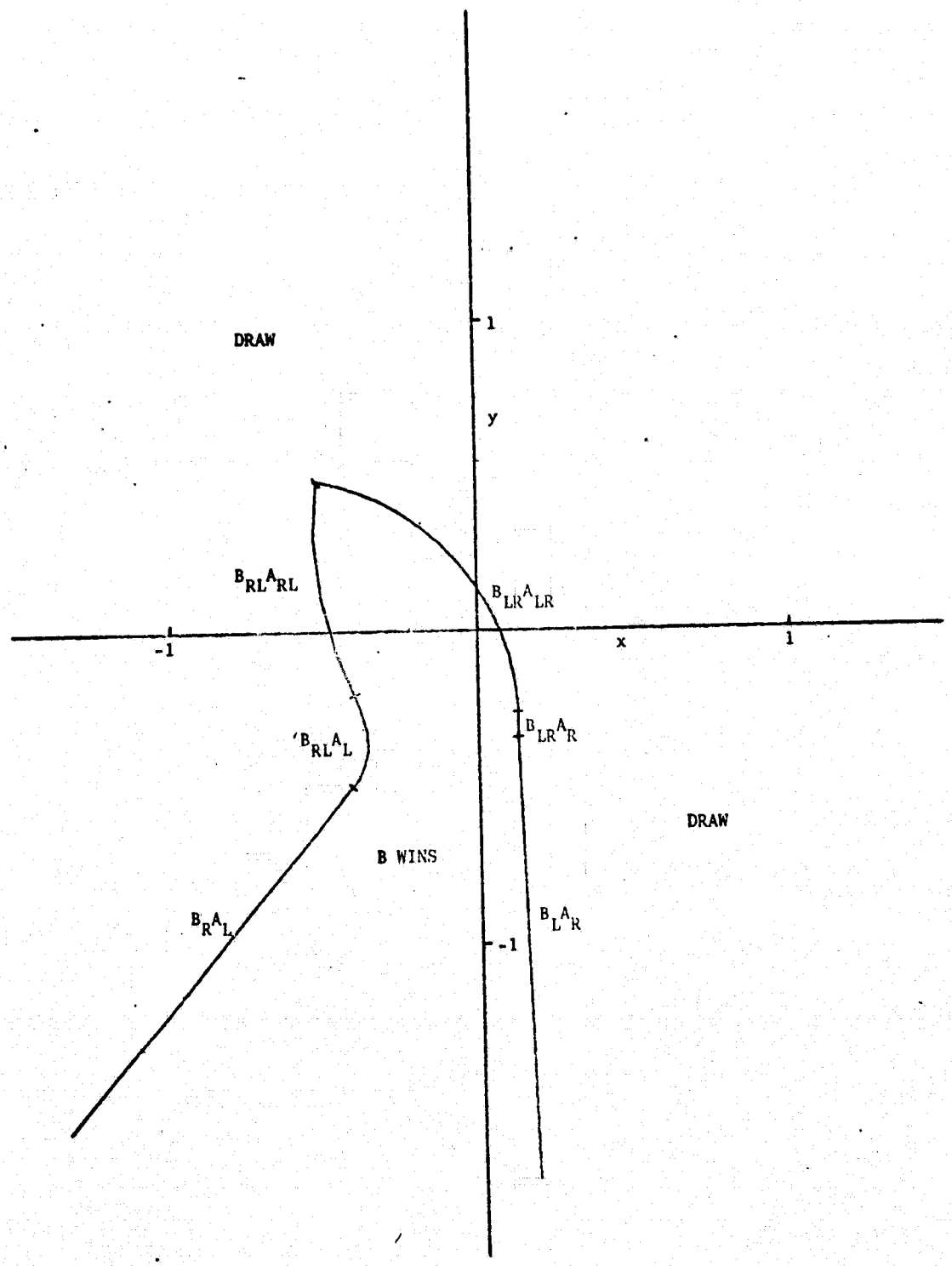

FIGURE 5.1(f). CAPTURE REGIONS, H = 40^{o}

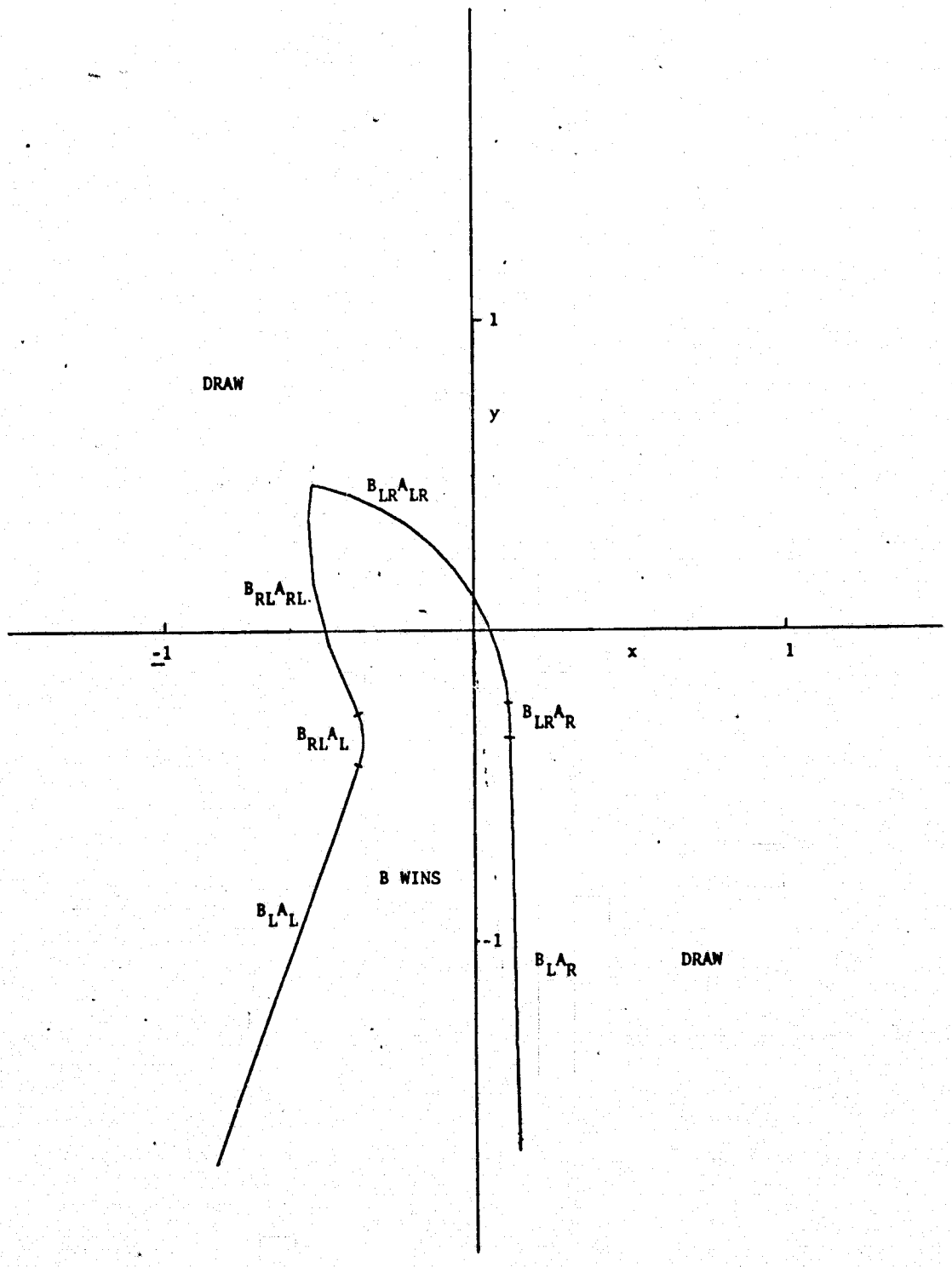

FIGURE 5.1(g). CAPTURE REGIONS, H = 42^o

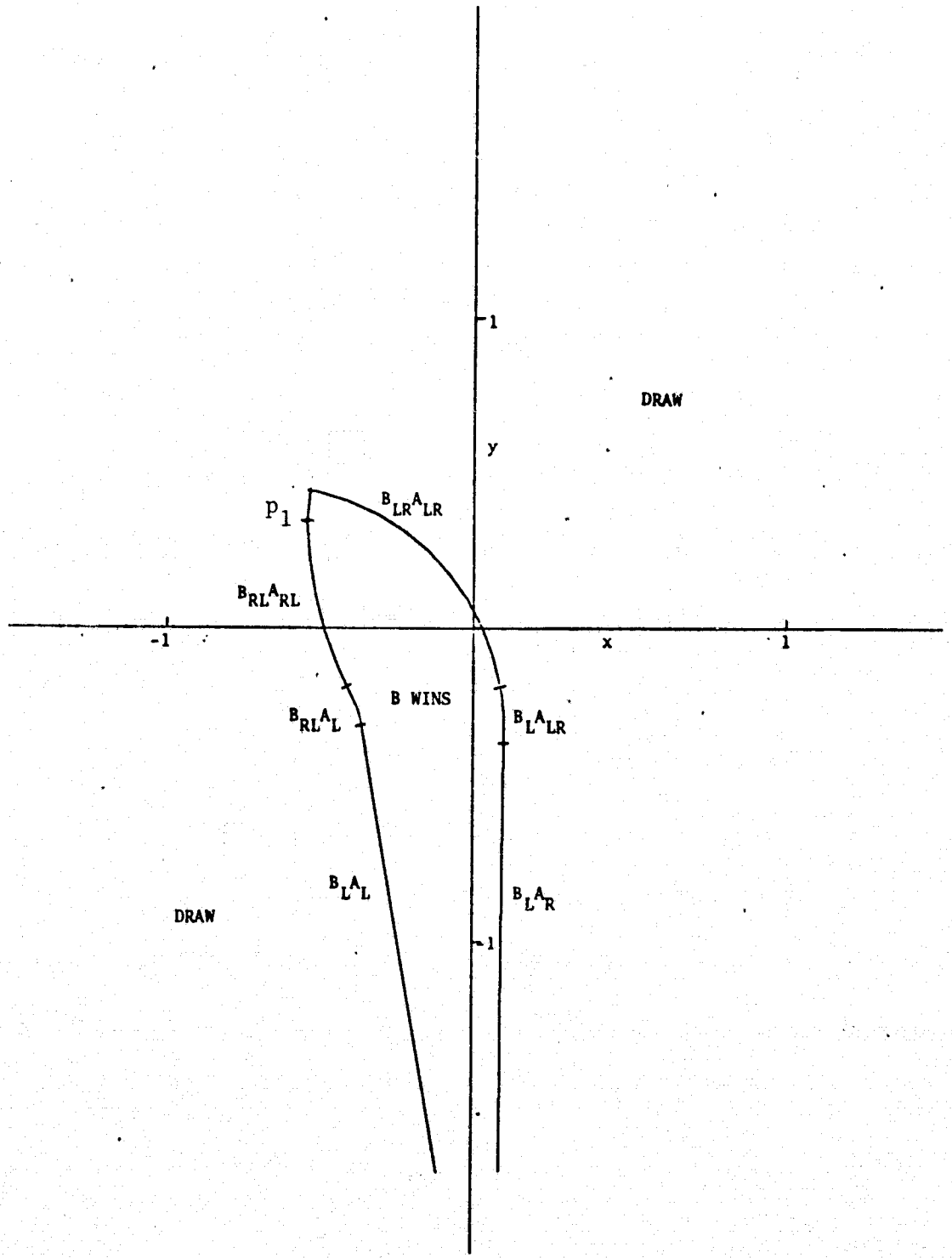

FIGURE 5.1(h). CAPTURE REGIONS, H = 45^o

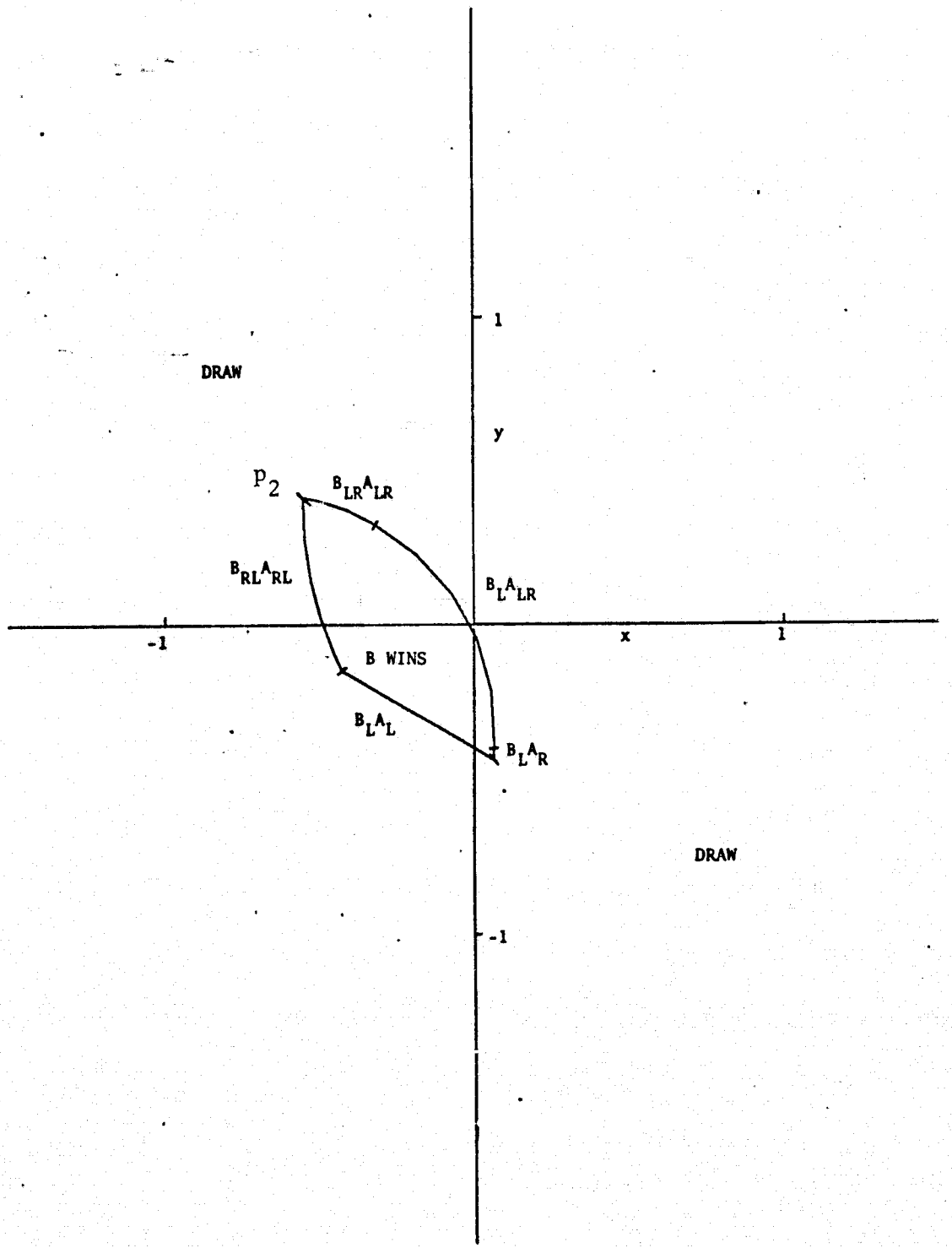

FIGURE 5.1(i). CAPTURE REGIONS, H = 50^o

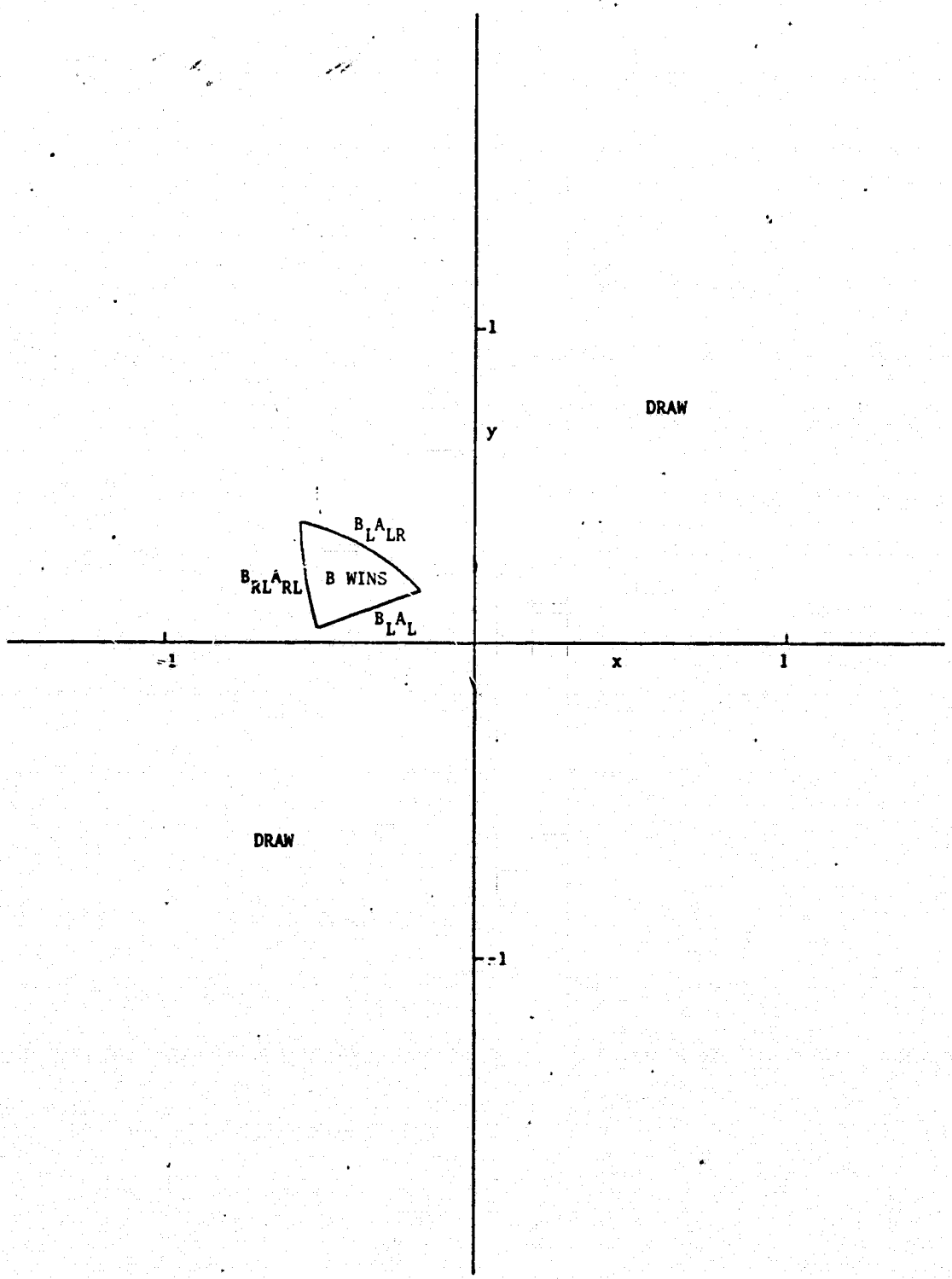

FIGURE 5.1(j). CAPTURE REGIONS, H = 55°

the region far behind A should be bounded, since A can readily increase the relative range, when the initial range is greater than B's effective weapon range.

For the speeds and turn rates which have been chosen, neither aircraft encounters a singular arc[23, p 32], and neither aircraft switches more than once. The parametric conditions under which these phenomena do occur therefore remain as an open question, the answer to which could require a considerable extension of the present results. Presumably, extremely high relative turn rates would increase the proportion of the time spent in straight flight. Because the combat model termination condition requires that each pursuer control both the relative position and the relative heading, using only one control input (the turn rate), it is fairly obvious that the draw condition should be the most frequent outcome. It is also evident that speed is often a disadvantage, for both pursuer and evader, and that sharp turns are the only means available for "reducing" the speed in a given direction.

Each point shown on these barrier plots is a possible initial condition associated with a specific optimal pursuit-evasion trajectory pair and a specific end condition. The real-space trajectories are given by the associated parameter values, as computed for the barrier. For example, the maneuvers associated with a barrier point x_o, y_o, H_o might be $B_{RL}A_{RL}$, for which τ_A, τ_B and τ are computed and printed as output values, implementing the analytical results described in earlier pages of this report. These figures imply that A turns right from the initial state (0, 0, 0) until the time $t = \tau - \tau_A$, while B turns right from the initial state (x_o, y_o, H_o) until the time $t = \tau - \tau_B$. The paths can then be drawn in real space over the remaining time, after which the relative state must correspond to the end

condition which had been assumed in deriving the maneuvers $B_{RL}A_{RL}$. A typical trajectory pair of this type is chosen to correspond to the point labelled "p_1" in Fig. 5.1(h). The associated computer output is

$x = -.545$	$\tau_A = 1.206$	$x_f = -.442$
$y = .347$	$\tau_B = 1.213$	$y_f = -.526$
$H = 45°$	$\tau = 1.698$	$H_f = 40°$

The real space paths are as shown in Fig. 5.2, which can be drawn using the first 6 of these numbers, together with the turn

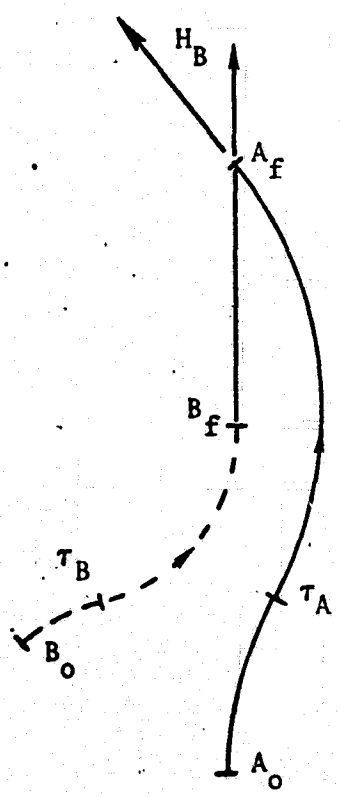

Initial Condition
From Fig. 5.1(h)

Fig. 5.2 Representative Barrier Maneuvers in Real Space

radii, $R_A = 1$, $R_B = .4545$. Notice that the end conditions show A ahead of B at the relative heading $H_B = 40°$, as required, and that the entire trajectory in relative space occurs on the closed contour corresponding to B's barrier.

Another interesting set of real-space maneuvers can be drawn from a "dispersal point", as shown for the heading H = 50° in Fig. 5.3. The initial condition is chosen at the point "p_2" in Fig. 5.1(i). Here, the evading vehicle A must immediately choose

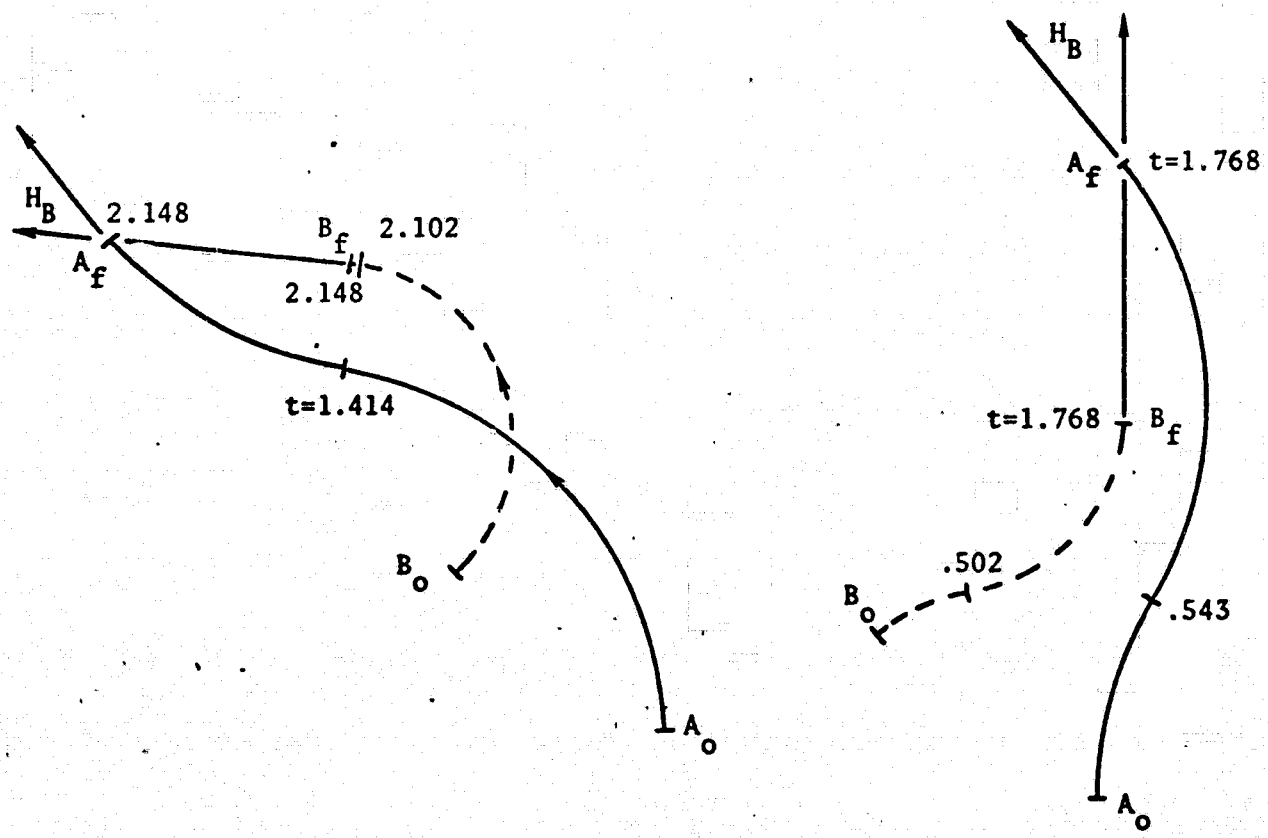

a) $B_{LR}A_{LR}$ b) $B_{RL}A_{RL}$

Fig. 5.3 Dispersal Point Maneuvers in Real Space

between A_{LR} and A_{RL}, and B's maneuvers will depend on this choice. By so turning, A can keep the final angle-off at 40° or more, depending only upon whether B pursues optimally.

The performance of combat aircraft can be quantitatively measured in terms of the pursuer's optimal capture regions as found with respect to an optimally flown controlled evader. The capture regions of both A and B must depend upon all of the parameters, and the sensitivity to variations in these parameters can be found by making small changes in them, and by then recomputing the kill-regions with the new values of the parameters. A typical example of such a study is given in Fig. 5.4, which shows B's capture region dependence on the angle-off, H_B. The capture-region contours do not intersect each other, since increases in H_B can only increase B's capture region. On the other hand,

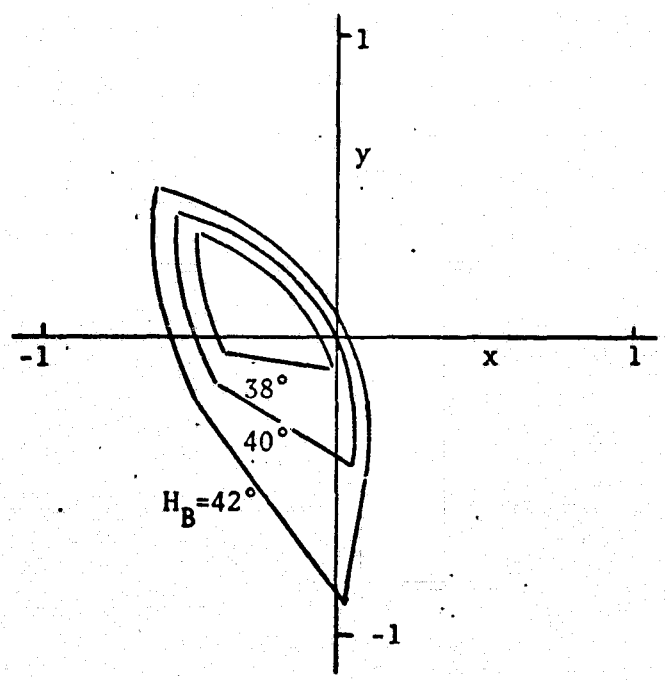

Fig. 5.4 Capture Region Dependence on H_B (H = 50°)

for example, increases in V_B could either increase or decrease B's capture region, depending upon the relative position and heading. A variational study of all six independent parameters (V_A, V_B, $\omega_{A_{max}}$, $\omega_{B_{max}}$, H_A, H_B) in the tail-chase version of the aerial combat problem has not been attempted, and could obviously involve a considerable computational effort.

6.0 CONCLUSIONS

The present differential-game version of the aerial combat problem brings together the six most important vehicle performance parameters (V_A, V_B, $\omega_{A_{max}}$, $\omega_{B_{max}}$, H_A, H_B) and the two most important pilot controls (ω_A, ω_B) as functions of the three most important geometric state variables (x, y, H). It is obvious that all of these eleven quantities should have some relevance both to the roles and to the maneuvers of both aircraft, and that only rather complex models of this type can be expected to provide meaningful results of general utility.

Designers and pilots of a particular combat aircraft are naturally interested in knowing the regions of the flight envelope in which this aircraft "is better than" a certain enemy aircraft. Since the outcome of an aerial combat encounter obviously depends not only upon the performance capabilities of both aircraft but also upon the weapon system characteristics, the initial conditions of the encounter and the maneuvers chosen by both pilots, the question can be answered only when all of these variables are specified. That is, for example, all aircraft must fly defensively from some relative initial conditions, and realistically, these initial geometries are subject to controlled change only when both vehicles apply finite accelerations to their trajectories.

General comparative statements concerning two combat aircraft are possible only when the important parameters are known for both of them at a number of flight conditions (Mach number and altitude). At each of these flight conditions, the capture regions of both aircraft can be found, and typically one will be larger (in terms of range, bearing and heading) than the other. Even when the aircraft and the capture

regions are identical, of course, the vehicle or pilot with knowledge of the optimal offensive-defensive maneuvers will have a considerable advantage over the other, whether his role is that of pursuer or evader.

It is suspected that the most useful results obtainable from a study of the present type relate to the defensive maneuvers of the aircraft, for the following reasons.

Since each aircraft in a one-on-one encounter has a bounded capture region, and since all aerial combat encounters begin with neither aircraft in the capture region of the other, optimal defensive maneuvers by either aircraft can always prevent the other from obtaining an advantageous relative position. For this interpretation of aerial combat, it appears that kills can occur only when:

i) One vehicle pilot (A) is unaware that the other (B) is nearby, or

ii) Both pilots are aware of the other, but at some point, one of them (A) maneuvers incorrectly, allowing the other (B) to enter the region "B Wins" as shown in Fig. 5.1, from which there can be no escape unless B subsequently maneuvers incorrectly.

7.0 REFERENCES

1. R. Isaacs, Differential Games, Wiley and Sons, 1965.

2. G. J. Olsder and J. V. Breakwell, "Role-Determination in an Aerial Dogfight," International Journal of Game Theory, Vol. 3, No. 1, pp. 47-66.

3. A. L. Leatham and U. H. Lynch, "Two Numerical Methods to Solve Realistic Air-to-Air Combat Differential Games," paper 74-22, AIAA 12th Aerospace Sciences Meeting, Washington, D.C., Jan. 30, 1974.

4. D. S. Hague, R. T. Jones and C. R. Glatt, "Combat Optimization and Analysis Program, COAP," Air-to-Air Combat Analysis and Simulation Symposium, Kirtland AFB, New Mexico, February 1972.

5. T. R. Harvey and J. D. Dillow, "Application of an Optimal Control Pilot Model to Air-to-Air Combat," paper presented at IEEE Conf. on Human Operator Modelling, 1968.

6. G. H. Burgin and L. J. Fogel, "Air-to-Air Combat Tactics Synthesis and Analysis Program Based on an Adaptive Maneuvering Logic," paper presented at Air-to-Air Combat Analysis and Simulation Symposium, Kirtland Air Force Base, N.M., February 29, 1972.

7. T. K. Campbell, T. T. Gold, R. H. Andrews and W. Moore, "Application of Performance Optimization Techniques to Tactical Aircraft Operations" (U), AFFDL-TR-70-41, Vol. II, August 1970 (SECRET).

8. Anon., "Air-to-Air Combat Analysis and Simulation Symposium," (U), AFFDL-TR-72-57, Vol. I and II, May 1972 (SECRET).

9. R. L. Simpson, et al, "Weapon System Effectiveness Analysis, Optimization and Simulation - Phase I, Autopilot Parameter Optimization," Technical Report AFATL-TR-71-20, Vol. VI, February 1971.

10. D. S. Hague, "Application of Combat Simulation Techniques to Guidance Law Determination in Aerial Combat," Aerophysics Research Corporation Technical Note TN-190, July 1973.

11. D. A. Roberts, "Aerial Combat Analysis Using Differential Games," paper presented at Air-to-Air Combat Analysis and Simulation Symposium, Kirtland Air Force Base, New Mexico, February 29, 1972.

12. D. A. Roberts and R. C. Montgomery, "Development and Application of a Gradient Method for Solving Differential Games," NASA TN D-6502, 1971.

13. A. W. Merz, "The Homicidal Chauffeur," AIAA Journal, Vol. 12, No. 3, March 1974; also Stanford University, Department of Aeronautics and Astronautics Rep. 418, March 1971.

14. S. M. D. Williamson-Noble, "Singular Surfaces in Aircraft/Aircraft Differential Games, Assuming a Spherical Acceleration Vectogram for Each Aircraft," 5th Hawaii International Conference on System Sciences, 1972.

15. W. L. Othling, "Application of Differential Game Theory to Pursuit-Evasion Problems of Two Aircraft," (Dissertation) DS/MC/67-1, WPAFB, Ohio, June 1970.

16. U. H. D. Lynch, "Differential Game Barriers and Their Application in Air-to-Air Combat," (Dissertation) DS/MC/73-1, WPAFB, Ohio, March 1973.

17. W. Y. Peng and T. L. Vincent, "Some Aspects of Aerial Combat," AIAA Journal, Vol. 13, No. 1, January 1975.

18. A. W. Merz, "The Game of Two Identical Cars," Journal of Optimization Theory and Applications, Vol. 9, No. 5, May 1972.

19. W. W. Willman, "Formal Solutions for a Class of Stochastic Pursuit-Evasion Games," Technical Report No. 575, Division of Engineering and Applied Physics, Harvard University, Cambridge, Mass., November 1968.

20. Y. C. Ho, et al, Ed., "Proceedings of the First International Conference on the Theory and Applications of Differential Games," Univ. of Massachusetts, Amherst, Mass., September 29, 1969.

21. J. A. Sorensen, et al, "Final Report, Collision Avoidance System Analysis - U.S. Maritime Administration," Systems Control, Inc., Palo Alto, California, July 1975.

22. A. W. Merz and J. S. Karmarkar, "Collision Avoidance Systems and Optimal Turn Maneuvers," The Journal of Navigation, Vol. 29, No. 2, April 1976.

23. A. W. Merz, "Application of Differential Game Theory to Role-Determination in Aerial Combat," NASA CR-137713, July 1975.